Bioapplication of nanosemiconductors

by Ying Wang, Zhiyong Tang, and Nicholas A. Kotov*

Advances in semiconductor nanocolloids have provided a new set of materials with unique optical and electrical properties, which recently have grabbed biologists and biomedical engineers' attention for applications such as biolabels, biosensors, and image-contrast agents. These nanosemiconductors have also been used to fabricate devices for applications such as drug delivery and medical therapeutics. In this review, we introduce some of the latest examples of semiconducting nanostructures that have been applied successfully to problems in biotechnology, with a special focus on biosensing and bioimaging. We first describe how to take advantage of the optical properties of semiconductor quantum dots in these two research fields. In addition, we give a brief introduction to biosensors based on field-effect transistors (FETs) made of one-dimensional semiconductor nanowires and carbon nanotubes. Finally, we discuss the future development of semiconductor nanomaterials in the biological field.

Departments of Chemical Engineering, Biomedical Engineering, and Materials Science and Engineering,
2300 Hayward, H. H. Dow Building,
University of Michigan,
Ann Arbor, Michigan 48109, USA
*E-mail: kotov@umich.edu

Rapid advances in nanotechnology and nanoscience have provided a variety of nanoscale materials with highly controlled and unique optical[1-6], electrical[7-11], magnetic, or catalytic properties. The diversity in composition (inorganic or organic, metals or semiconductors), shape (particles, rods, wires, tubes, cubes, tetrapods, or triangles), and the readiness for surface functionalization (physical, chemical, or biological) has enabled the fabrication of various functional nanoscale devices[4,5,12-14]. Biologists have recently begun to borrow these nanotools and apply them to a variety of applications ranging from diagnosis of disease to gene therapies. Integration of biomaterials (e.g. proteins[15,16], peptides, or DNA[17,18]) with semiconductor quantum dots (QDs) and metal nanoparticles (NPs) greatly expands the impact of biophotonics and bioelectronics, particularly in optical imaging and biosensing, as well as therapeutic strategies[19-21]. Similarly, the conjugation of magnetic nanocolloids with biomaterials has led to the development of biological separation and purification, hyperthermia, and magnetic resonance imaging techniques. In addition, the similarity of size scale between nanomaterials and typical biomolecules makes these nanostructures particularly attractive for intracellular tagging and ideal for bioconjugation, such as antibody targeting of contrast agents.

ISSN:1369 7021 © Elsevier Ltd 2005

In comparison with NPs, the integration of one-dimensional nanostructures with biological systems to form functional assemblies has been slow until recently, as it has been hindered by the difficulties associated with the synthesis and fabrication of these materials with well-controlled dimensions, morphology, phase purity, and chemical composition. Thanks to research efforts, different methods of synthesizing one-dimensional nanowires (NWs) and carbon nanotubes (CNTs) have been developed in the last few years[22-24]. With such synthetic techniques in hand, one-dimensional nanostructures should find applications in the construction of novel nanoscale devices, such as biosensors, which combine the conductive or semiconductive properties of the nanomaterials with the recognition or catalytic properties of biomaterials. One type of sensor system, based on the concept of field effect transistors, has attracted much attention recently. Sensing devices made of semiconductor nanostructures, such as semiconductor single-walled carbon nanotubes (SWNTs)[25-27] and Si[28], SnO_2[29], ZnO, and In_2O_3 NWs[30], can generally be understood in terms of change in the surface charge of the nanostructure with the adsorption or desorption of molecular species. Because of the high surface-to-volume ratio of the one-dimensional nanostructures, their electronic conductance may be sensitive enough to the surface species so that single-molecule detection becomes possible.

Applications of one-, two-, or three-dimensional nanostructures can benefit substantially from various bioconjugation techniques. The broad field of bioconjugation chemistry and the richness in surface chemistry of nanomaterials enables biological and nonbiological systems to be merged at the nanoscale.

In this review, we introduce some recent examples of nanostructures that have been successfully applied to problems in biotechnology. We focus on semiconductor nanomaterials, but information on the biological application of metal and magnetic nanocolloids can be found elsewhere[31-37]. The use of semiconductor QDs as fluorescence labels in bioimaging and biosensing, which is the most intensively studied system and may be the first practical application in the near future, is described. Also, we give a brief discussion of biosensors based on field-effect transistors made of semiconductor NWs and CNTs. Several examples of metal NPs are also given to compare semiconductor and metal nanomaterials in biological applications.

Bioimaging using quantum dots

Semiconductor QDs, also called semiconductor nanocrystals, are generally composed of atoms from groups II and VI or III and V of the periodic table. The nanoscale size of QDs leads to the quantum-confinement effect, which results in interesting optical and electronic properties. The unique photophysical properties of inorganic nanomaterials provides a new class of biological labels that could overcome the limitations of conventional organic fluorophores. QDs show size-tunable fluorescence emission and have a narrow and symmetric spectral line profile (the full width half maximum is typically 25-35 nm) compared with organic dyes, making QDs ideal for simultaneous detection of multiple fluorophores by excitation of a single light source[38,39]. Photoluminescence lifetimes are long (~20-50 ns), which allows imaging of living cells without interference from background autofluorescence. Stability against photobleaching[40], large molar extinction coefficients, high quantum yield[41], and large surface-to-volume ratios make QDs superior to organic fluorophores in detection sensitivity as well as in long-term tracking of biological processes. Here, we describe some recent examples of using semiconductor QDs as biological imaging agents.

The first milestone application of QDs as luminescence labels in bioimaging was reported by Alivisatos' group, which demonstrated the multicolor labeling of fixed mouse 3T3 fibroblasts[2]. Since as-prepared CdSe/ZnS QDs in trioctylphosphine/trioctylphosphine oxide (TOP/TOPO) are only soluble in nonpolar solvents and are toxic, a silica shell was intentionally coated onto the nanocrystals, followed by coupling of ligands to the silica. The ligands on the silica surface were subsequently used in bioconjugation. Biotinylated QDs with red photoluminescence selectively stained cytoskeletal filaments modified with streptavidin. Green-emitting QDs with trimethoxysilylpropyl urea and acetate groups showed high affinity to the cell nucleus (Fig. 1). Constant excitation of bioactive QDs over 4 hours with an Ar^+ laser resulted in constant emission with little decay.

Almost at the same time, Chan and Nie prepared water-soluble CdSe QDs by surface exchange of the organic ligands for mercaptoacetic acid, which can offer pendant carboxylic acid groups for further coupling[41]. CdSe QDs that were labeled with the protein transferrin underwent receptor-mediated endocytosis in cultured HeLa cells, and those QDs that were labeled with immunomolecules recognized specific

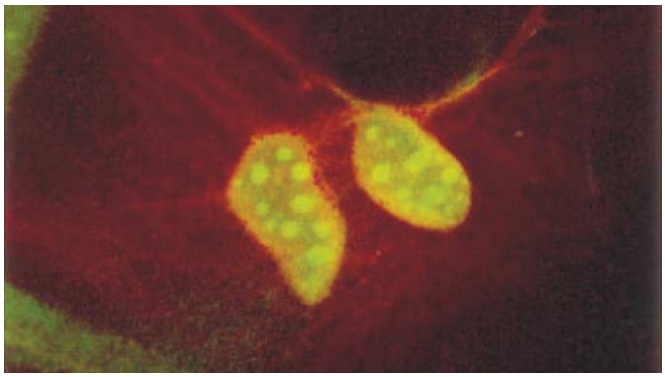

Fig. 1 Mouse 3T3 fibroblast labeled with CdSe quantum dots. (Reprinted with permission from[2]. © 1998 AAAS.)

antibodies or antigens. These two papers reported in 1998 laid the foundation of QDs as biolabels and opened the door to biological applications of semiconductor NPs.

Successful imaging of live cells with semiconductor QDs as labels in the following years has further promoted the popularity of using QDs in biological systems[42-44]. Impressive progress has been achieved in cancer imaging using semiconductor nanocrystals. In 2003, Wu *et al.*[40] conjugated immunoglobulin G (IgG) and streptavidin to CdSe QDs with different emission spectra to label the breast cancer marker Her2 on the surface of fixed and live cancer cells. They also used the conjugated nanoparticles to stain actin and microtubule fibers in the cytoplasm, as well as to detect nuclear antigen inside the nucleus. This work aims to identify tumors that are likely to respond to an anticancer drug, although current testing procedures indicate that it is possible some tumors that are sensitive to drugs are missed. Although *in vitro* assays using QDs as biolabels may provide details of molecular interactions under experimental conditions, the complexity of the physiological environment found in live animals is absent. The recent upsurge of *in vivo* studies has proved that QDs are just as effective here as in the test tube. Ballou *et al.*[45] have observed the circulation and accumulation processes of polyethylene glycol-stabilized CdSe QDs in mice blood vessels. Gao and coworkers[46] have combined CdSe QD targeting and imaging in live animals. QD probes encapsulated in a triblock copolymer could be delivered to tumors by both passive and active targeting mechanisms. In passive mode, macromolecules around the particles and the nanocrystals accumulated preferentially at the tumor sites through an enhanced permeability and retention effect. In active tumor targeting, antibody (Ab)-conjugated QDs targeted a prostate-specific membrane antigen (PSMA) on the tumor. Intense signals were obtained by injecting antibody probes, QD-PSMA-Ab, into the tail vein of a tumor-bearing mouse (Fig. 2). One advantage of this design comes from the hydrophilic polymer with a large number of functional groups, allowing attachment of both diagnostic and therapeutic agents. Such multifunctional dots could target cancer cells, followed by drug release triggered by laser light, so that only tumor cells receive the toxin, minimizing side effects.

Work has not been confined to static imaging. Kinetic studies on the mobility of human mammary epithelial tumor cells and nontumor cells has been conducted[47]. Thin layers of silica-capped CdSe/ZnS NPs were deposited on collagen-coated substrates, followed by the plating of cells. As tumor cells pass through the substrate, they engulf luminescent QDs and leave behind a phagokinetic track free of QDs that is no longer luminescent. Additionally, the results confirm that cancer cells are both invasive and migratory, while noncancer cells are noninvasive and relatively immobile. Based on a similar idea, Pellegrino and coworkers[48] have compared the behavior of seven different adherent human cell lines and observed two distinct types of behavior of cancer cells; they either leave long fluorescent-free trails (Fig. 3a) or clear zones of varying sizes around the periphery of the CdSe/ZnS films (Fig. 3b), which is believed to be related to the invasiveness of the cancer cells. Among cancer cell lines known to move around the body, even those that cannot be detected by a membrane get caught by QDs. Voura *et al.*[49]

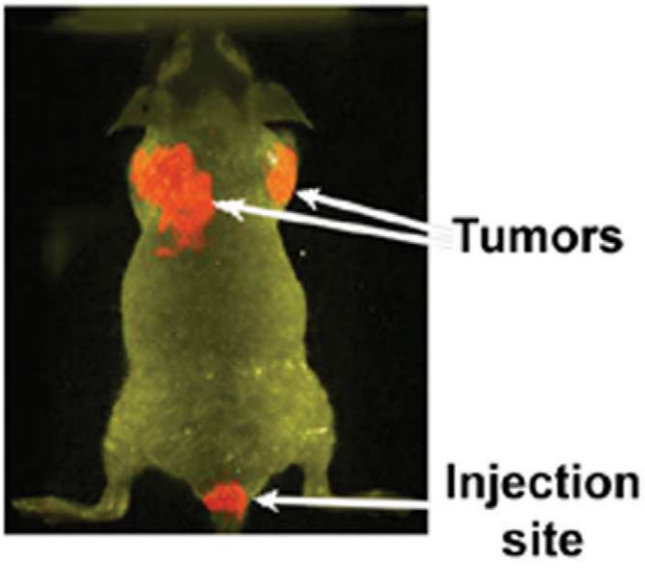

Fig. 2 In vivo fluorescence images of tumor-bearing mice using QD probes conjugated to PSMA-Ab. (Reprinted with permission from[46].)

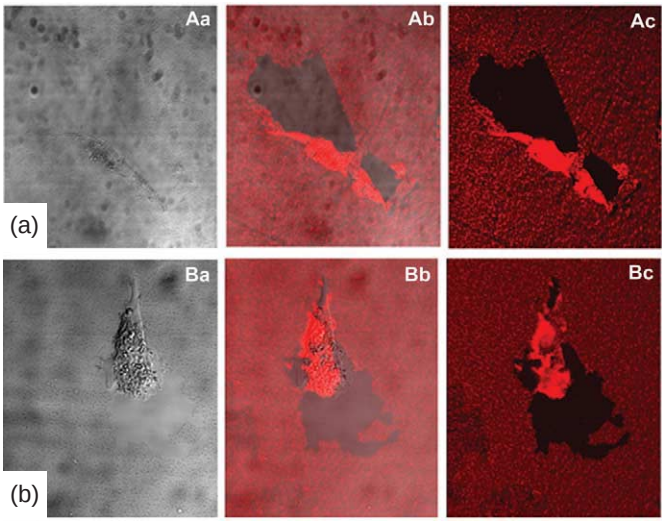

Fig. 3 Phagokinetic tracks in (a) the highly metastatic human mammary gland adenocarcinoma cell line MDA-MB-231 and (b) cell line SW480, grown on a collagen substrate coated with a layer of fluorescent semiconductor nanocrystals. Images were collected with a confocal microscope using a fluorescence detector to record the nanocrystal trails (Ac, Bc) and a transmitted light detector to visualize the cells (Aa, Ba); the merged pictures (Ab,Bb) colocalize the cells and the nanocrystal layer. After 24 hours, sizable regions free of nanocrystals, larger than the cells themselves, are detected in (a) and a small area free of nanocrystals surrounding the cell (b). (Reprinted with permission from[48]. © 2003 Blackwell Publishing.)

have tracked the extravasation of metastatic tumor cells into surrounding tissues using nanocrystals and fluorescence emission scanning microscopy. After injection into the tail vein of mice that are syngeneic, tumor cells labeled with QDs were extravasated into lung tissues and other organs, but these cells did not regularly form tumors in those organs. This work enables the study of not only extravasation and invasion mechanisms of tumor cells into tissues in real time, but also a variety of other multicellular interactions that occur during growth and development processes in animals. For example, Dubertret *et al.*[50] have demonstrated that, after injection into *Xenopus* embryos, the luminescence of CdSe QDs stabilized by phospholipid block-copolymer micelles could be followed to the tadpole stage, allowing long-term tracking experiments in embryogenesis.

With increasing demand for imaging structures deep inside the body, scientists are directing their attention to QDs that emit in the near-infrared region (NIR, 650-1000 nm), a region where transmission of light through tissues and blood is maximal. Theoretical studies show that long-wavelength adsorption by biological tissue minimizes the background noise, since cellular autofluorescence is greatly reduced[51]. Synthetic scientists have successfully prepared NIR QDs with tunable photoemission, such as HgTe[52], CdHgTe, PbSe[53], InP, and InAs[54] for possible biological applications. Recently, Kim *et al.*[55] made a key advance in cancer imaging using CdTe/CdSe core/shell QDs. CdTe/CdSe NPs have a staggered band structure, and hence are referred to as type II QDs. The excited holes and electrons reside in the CdTe core and CdSe shell, respectively, and the QDs emit in the NIR region of the spectrum. The QDs coated with an oligomeric phosphine have a hydrodynamic diameter of 15.8 nm, which is an ideal size for the retention of QDs in the sentinel lymph node (SLN). The dots were used in lymph mapping, which is a major procedure in cancer surgery. When injected into a large animal (400 pmol into a 35 kg pig), a surgeon was able to follow lymphatic flow toward the SLN in real time and to identify the position of the SLN, about 10 mm under the skin, within minutes (Fig. 4). Precise resection was achieved under the guidance of strong luminescent images. Owing to the greater photostability of QDs over conventional IR-emitting dyes, the surgeon can even inspect the site after surgery with high sensitivity to ensure completeness of the procedure.

Although this review focuses on bioimaging using luminescent semiconductor QDs, it is worth mentioning that high-contrast and high-resolution images with molecular specificity to cancer can also be achieved using metal

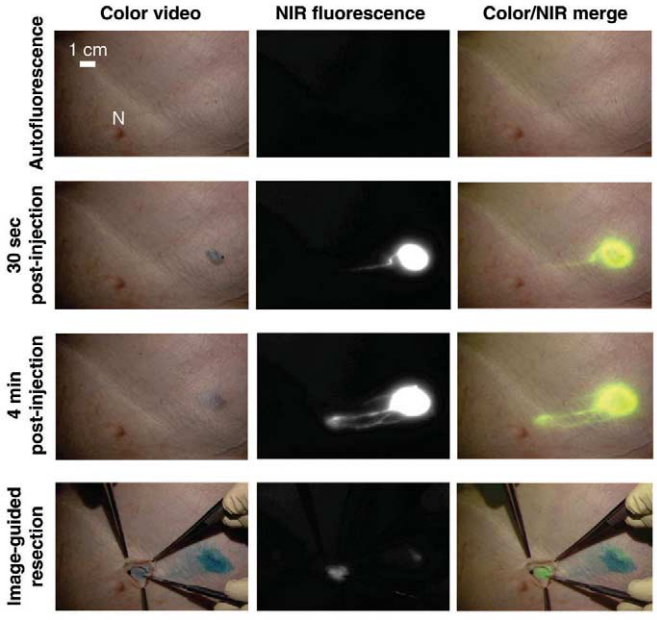

Fig. 4 Images of the surgical field in a pig injected intradermally with 400 pmol of NIR QDs in the right groin. Four time points are shown from top to bottom: before injection (autofluorescence); 30 s after injection; 4 min after injection; and during image-guided resection. For each time point, color video (left), NIR fluorescence (middle), and color-NIR merge (right) images are shown. Fluorescence images have identical exposure times and normalization. To create the merged image, the NIR fluorescence image was pseudocolored lime green and superimposed on the color video image. The position of a nipple (N) is indicated. (Reprinted with permission from[55].)

NPs[20,21,56]. Recently, Copland *et al.*[57], in collaboration with our group, developed a molecular-based contrast agent composed of Au NPs conjugated to a monoclonal antibody to enhance specificity and sensitivity of optoacoustic tomography (OAT) analysis. This novel medical imaging method uses optical illumination and ultrasonic detection to produce deep-tissue images based on light adsorption. The strong optoacoustic signal of Au NPs with a surface plasmon resonance peak positioned at a desirable wavelength between 520 nm and 1300 nm makes the NPs ideal contrast agents for OAT imaging of deep tumors in the early stages of cancer or metastatic lesions. In a series of *in vitro* experiments, Herceptin (a monoclonal antibody (mAb) that binds HER2/neu) conjugated to 40 nm NPs (mAb/NPs) selectively targeted human SK-BR-3 breast cancer cells. The latter were detected and imaged in a gelatin phantom with embedded gel cylinders, which together optically resembled breast tissue (Fig. 5a). Optoacoustic images show that the embedded tubes filled with suspension of NPs (Fig. 5b, tube 2) or SK-BR-3 breast cancer cells incubated with mAb/NPs (Fig. 5b, tube 3) show a bright signal, while the negative control tube filled with the same gel as the surrounding medium is invisible to detection (Fig. 5b, tube 1). Sensitivity experiments show that a concentration as low as 10^9 NPs/ml are detectable at a depth of 60 mm, a detection depth that can not be achieved using pure optical technology.

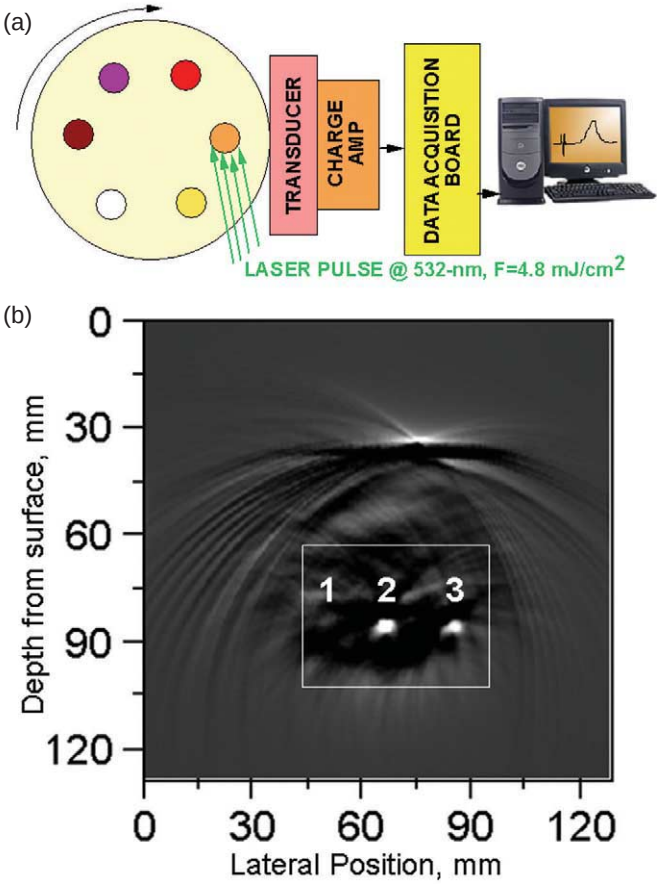

Fig. 5 Optoacoustic imaging of cells treated with mAb/NPs. (a) Schematic of a gelatin phantom with six embedded small gel cylinders loaded with Au NPs and the experimental setup for optoacoustic measurements. (b) Optoacoustic image of a gel phantom with three embedded tubes: Tube 1 is filled with the same media as the phantom gel (negative control), tube 2 is filled with NPs (10^9 NP/ml), and tube 3 is filled with SK-BR-3 cells treated with mAb/ NPs. Two of the three tubes can be clearly visualized. (Reprinted with permission from[57]. © 2001 Elsevier.)

Immunoassays using quantum dots

As with applications in bioimaging, the construction of biosensors for immunoassays using nanomaterials also involves bioconjugates. We believe that immunoassay biosensors are a logical extension of the imaging applications of nanostructures, since both exploit the dependence of nanomaterial properties on the attached biological ligands. The large difference originates from the characteristics of biosensors, which should have high sensitivity to external stimuli. Combining the functionality of biological molecules with the unique properties of nanostructures gives a new hybrid design for nanoscale devices.

Generally, current nanoscale biosensors can be divided into two categories, light-driven or electron-driven devices. For optical nanosensing, semiconductor QDs are particularly attractive because of their long-term photostability, allowing continuous real-time monitoring.

One method for using QDs in sensing is to create a donor/acceptor complex, which exhibits switching capability via fluorescence resonance energy transfer (FRET). QDs are promising FRET donors or acceptors because of their tunable adsorption/emission, and high FRET efficiency has been well documented with QDs connected to various acceptors[15,58]. Complexes are made by grafting complementary bioconjugates, i.e. antibody-antigen pairs, onto the surfaces of different luminescent CdTe NPs. Their interactions are then exploited[16]. For example, antigen (bovine serum albumin, or BSA) is conjugated to red-emitting CdTe NPs, while green-emitting NPs are attached to the corresponding anti-BSA antibody (IgG). The formation of a BSA-IgG immunocomplex results in FRET between the two different NPs: the luminescence of green-emitting NPs (550 nm) is quenched while the emission of the red-emitting NPs (615 nm) is enhanced. Such NP-protein superstructures, showing

competitive FRET inhibition, offer a promising protocol for immunoassays (Fig. 6). Based on the same idea, sensing devices using QDs as the FRET-donating portion of an inorganic-organic nanohybrid have been demonstrated in sugar detection[59-61]. One benefit of using QDs in immunoassays is the ability to excite and detect several labeled species simultaneously using a single light source (i.e. multiplexing). Using this concept, Goldman *et al.*[62] prepared bioinorganic conjugates made with highly luminescent semiconductor nanocrystals (CdSe/ZnS core/shell QDs) and antibodies to perform multiplexed fluoroimmunoassays. They demonstrate the simultaneous detection of up to four toxins from a single sample probed with a mixture of four QD-antibody reagents.

An interesting biosensor showing reversible FRET has been fabricated by connecting CdSe/ZnS core/shell QDs with a photoactivatable species that functions as the reversible FRET acceptor[63]. QDs are connected to photochromic 1',3-dihydro-1'-(2-carboxyethyl)-3,3-dimethyl-6-nitrospiro-[2H-1-benzopyran-2,2'-(2H)-indoline] (BIPS) via a bridge of maltase binding protein (MBP) (Fig. 7a). Exposure to ultraviolet (UV) light catalyzes the photoconversion of BIPS from the colorless spiropyran (SP) to the colored merocyanine (MC) form, which functions as the FRET acceptor and therefore modulates QDs emission (Fig. 7). The photoconversion is reversible, with white light converting MC back to the SP form. Quenching of QD emission at 555 nm and enhancement of BIPS emission at 650 nm via FRET appears upon exposure of the complex to UV light (Fig. 7b). Well-controlled, reversible switching events were demonstrated by alternating the illumination light source between white and UV light (Fig. 7c). Incorporation of an emission unit that can be modulated via a biological stimulus enables the creation of photochromically switched devices or sensors, where QD emission modulation presets the device below some predetermined critical threshold.

The detection limits of analytical processes based on FRET can be as low as 10 ppt with a linear dynamic range from 0.1 ppt to 1000 ppt[64,65]. For the purpose of sensors, FRET efficiency could be enhanced further by using luminescent NWs or nanostructures with high surface-to-volume ratios[66]. These advances could lead to powerful, compact sensors.

Except for optical nanosensing by FRET, other methods based on the photonic properties of semiconductor QDs have also attracted much research interest. One system worth mentioning is the use of a photochemical-reaction-induced photocurrent for biosensor applications. Pardo-Yissar and

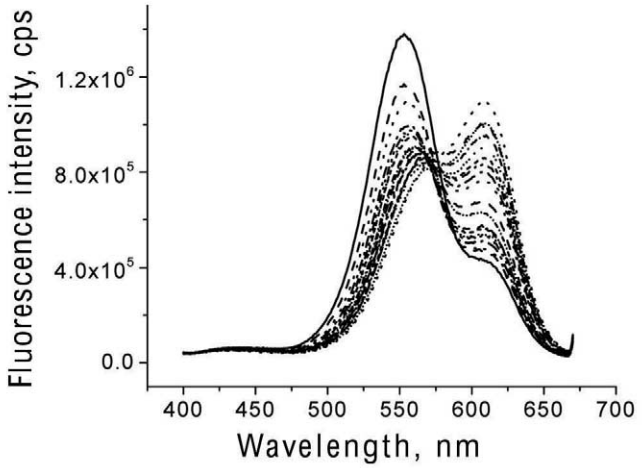

Fig. 6 Fluorescence emission spectra recorded at different times after mixing 10^{-7} M CdTe NP-BSA with 10^{-7} M CdTe NP-IgG. The intensity of the peak at 553 nm decreases with time while the intensity of the peak at 611 nm increases. (Reprinted with permission from[16]. © 2002 American Chemical Society.)

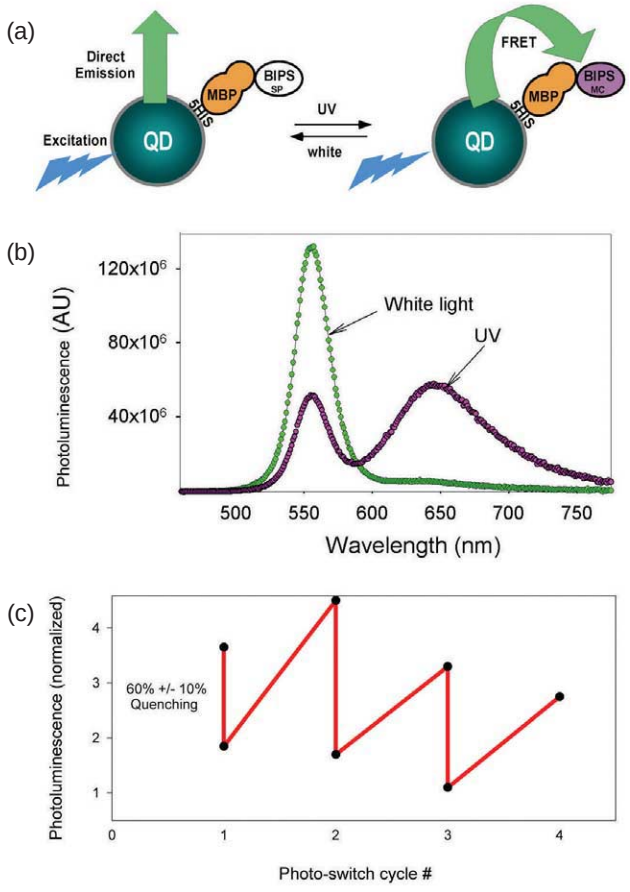

Fig. 7 (a) Schematic of QD modulation by MBP-BIPS. (b) Spectral properties and modulation function of MBP-BIPS and the 555 nm emitting QDs. (c) Monitoring of cyclical photoconversion effects on QD photoluminescence (photoluminescence monitored at 555 nm, starting with white light and switching to UV). (Reprinted with permission from[63]. © 2004 American Chemical Society.)

coworkers[67] have performed the first successful experiment, in which an acetylcholine esterase (AChE)/CdS QD hybrid system was constructed for the photoelectrochemical detection of AChE inhibitors. The CdS QDs were first covalently connected to a Au electrode, then covalently linked to the AChE. The CdS QD/AChE hybrid system is photoelectrochemically active in the presence of acetylthiocholine, which is transformed to acetate and thiocholine by AChE-catalyzed hydrolysis. The product of thiocholine acted as an acceptor for holes produced by excitation of the CdS QDs. This eliminates the radiative recombination of electron-hole pairs of QDs, so a steady-state photocurrent is generated. They also demonstrated that the addition of enzyme inhibitors decreases the photocurrents, so the nanoparticle/AChE system acts as a biosensor for the respective inhibitor. Such versatile photoelectrochemical labeling for different biosensors has potential for detecting biological warfare agents.

Other sensors using nanoparticles

Besides immunoassays, another biosensor research hotspot is the use of QDs to detect protein (e.g. nicotinamide adenine dinucleotide (NADH), glucose oxidase, or GOD), organic (e.g. ascorbic acid, cholesterol), or gas molecules (e.g. NO, CO) that are related to fundamental biological processes. Since Katz and Willner[37] have exclusively reviewed recent developments in this direction, just two examples are given here. Taking advantage of the layer-by-layer technique, various sensors with high sensitivity have been fabricated based on thin films made from metal or semiconductor NPs. Vossmeyer's group[68,69] has prepared thin films based on Au or Pt NPs to detect the resistance change on exposure to different vapors or gases. Sharing the same detection principle, Pinna *et al.*[70] have fabricated gas sensors using semiconductor metal oxides, SnO_2 and In_2O_3, and the sensors show considerable sensitivity and selectivity to NO_2 and CO.

Biosensors using one-dimensional nanostructures

NWs and CNTs can be used for direct, label-free, and real-time detection of biomolecule binding by taking advantage of their electrical properties. Here, we focus on FETs made of semiconductor NWs and SWNTs. Such FETs show potential for very high sensitivity since the depletion or accumulation of charge carriers, which are caused by the binding of a charged biological macromolecules on the surface of NWs or SWNTs, can affect the entire cross-sectional conduction pathway of these nanostructures.

Semiconducting Si NWs are a promising candidate, since the doping type and concentration can be controlled, which enables sensitivity to be tuned in the absence of an external gate. Studies on biosensors made from Si NWs can be traced back to pioneering work by Lieber's group, in which they demonstrated ultrasensitive detection of biological and chemical species by exploring nanoscale FETs[28]. Biotin-modified Si NWs were used to detect streptavidin at a concentration down to at least picomolar levels by monitoring the change in conductance of the NWs. In addition, antigen-functioned Si NWs show reversible antibody binding and concentration-dependent detection in real time. Shortly after this application was described, a series of tests was performed by the same group to detect specific DNA sequences[71,72]. They demonstrated that a 25 pM solution of target DNA could be detected on Si NWs with a 12-mer oligonucleotide attached, with excellent discrimination against single-base mismatches. The success of using NW FETs modified with receptors or ligands for specific detection leads to the point that the detection of a single entity (i.e. a single cell, virus, protein, and even DNA) becomes possible. Very recently, Patolsky *et al.*[73] fabricated Si NW FETs for electrical detection of single virus. This experiment is illustrated schematically in Fig. 8a. When a virus particle binds to the antibody receptor on a NW device, the conductance should change from the baseline value; when the virus unbinds, the conductance should return to the baseline value. For a *p*-type NW, the conductance should decrease (increase) when the surface charge of the virus is positive (negative). One key achievement in this report is the multiplexed detection of different viruses at the single particle level by modifying NWs in an array with antibody receptors specific either for influenza A (nanowire 1) or adenovirus (nanowire 2). Simultaneous conductance measurements were obtained when adenovirus, influenza A, and a mixture of both viruses were delivered to the devices. As the charged viruses pass over the Si NWs, the specific binding/unbinding behavior of the viruses is readily distinguished from rapid diffusion processes by the duration of the conductance change. Diffusion gives a much shorter duration of 0.4 s (red and blue arrows) compared to 16 ± 6 s in specific, controlled assembly (Fig. 8b). Addition of influenza A to NW1 (blue) modified

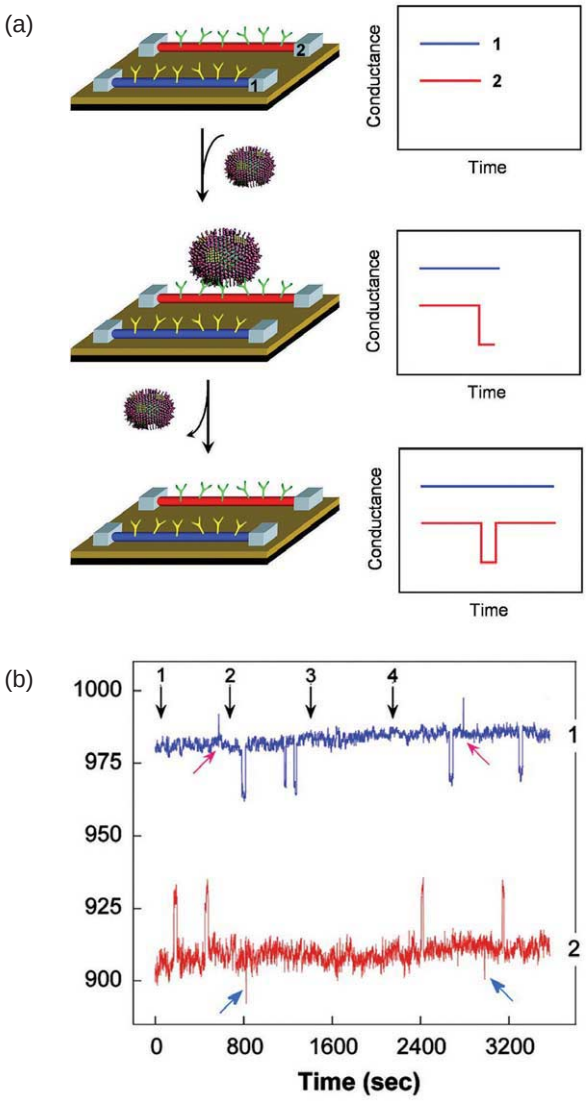

Fig. 8 (a) Nanowire-based detection of single viruses. (b) Conductance versus time data, recorded simultaneously from two Si nanowires elements; one nanowire (nanowire 1) was modified with anti-influenza type A antibody (blue), and the other (nanowire 2) with anti-adenovirus group III antibody (red). Black arrows (1-4) correspond to the introduction of adenovirus, influenza A, pure buffer, and a 1:1 mixture of adenovirus and influenza A. Small red and blue arrows highlight conductance changes corresponding to diffusion of viral particles past the nanowire and not specific binding. (Reprinted with permission from[73]. © 2004 National Academy of Sciences, USA.)

with anti-influenza A antibody yields a negative conductance change, while binding of negatively charged adenovirus to the receptor on NW2 (red) modified with anti-adenovirus antibody gives a positive conductance change.

Similarly, CNTs have also shown that the electrical conductance of such one-dimensional nanosemiconductors is highly sensitive to their environment and varies significantly with changes in electrostatic charges through the surface adsorption of various molecules[25,74]. Unlike Si NWs, CNTs show structurally defined semiconductive or conductive forms, but only semiconducting nanotubes exhibit a large conductance change in response to the electrostatic and chemical gating effects desired for FETs. It is well known that around 70% of as-prepared SWNTs are semiconducting, so the SWNTs demonstrating semiconductor-like behavior (i.e. where the conductance can be sensitively gated by applied voltage) should be selected as sensors. Research on biomodified SWNTs has demonstrated the selective detection of proteins in solution via specific antigen and antibody interactions[75]. One example is a diagnostic assay that details affinity binding of an antibody to U1A RNA splicing factor immobilized on SWNTs, which is a prominent auto-antigen target in systemic lupus erythematosus and mixed connective tissue disease[75]. U1A was covalently conjugated to Tween-coated SWNTs, and binding of antibodies was simultaneously monitored using a quartz crystal microbalance (QCM) and electronic measurements on SWNTs that bridged two electrodes. The addition of 10E3, a mAb that specifically recognizes U1A, resulted in an abrupt decrease in the conductance versus time curve for antibody concentrations as low as 1 nM (Fig. 9). In contrast, mAbs 3E6 and 6E3 specific for structurally related but different RNA-binding autoantigens did not recognize U1A in this assay, confirming the immunosensing selectivity. The system demonstrates the electronic detection of the antibody-antigen interactions at 100-fold higher sensitivity than the QCM.

The smart combination of the specificity of interaction between biological molecules and the flexibility to functionalize CNT surfaces makes it possible to fabricate SWNT-FETs. The CNTs can be assembled in contact with Au electrodes via a three-strand homologous recombination reaction between a double-stranded DNA (dsDNA) molecule serving as a scaffold and an auxiliary single-stranded DNA (ssDNA)[76]. RecA proteins are first polymerized on the auxiliary ssDNA molecules that have an identical sequence to the dsDNA (Fig. 10c, step i), which then bind to the scaffold dsDNA molecules (Fig. 10c, step ii). A streptavidin-functionalized SWNT is guided and immobilized to the dsDNA molecule using antibodies bound to RecA and biotin-streptavidin-specific binding (Fig. 10c, step iii). Ag wires are formed by reduction of Ag salts (Fig. 10c, step iv) and subsequent electroless Au plating covers the ends of the CNT to form two contact electrodes (Fig. 10c, step v, Fig. 10a). Although the authors only present the basic field-effect

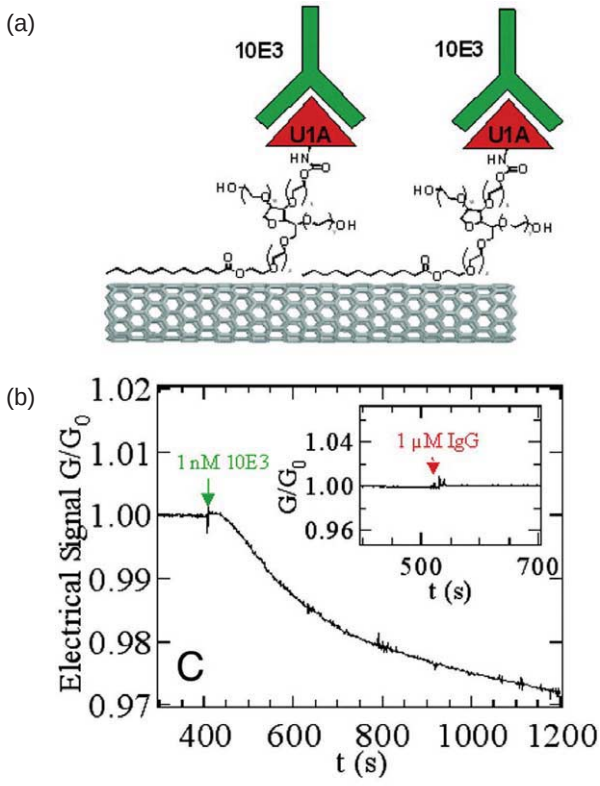

Fig. 9 (a) Scheme for specific recognition of 10E3 mAb with a nanotube device coated with a U1A antigen-Tween conjugate. (b) Conductance versus time curve of a device shows specific response to 1 nM 10E3. (Reprinted with permission from[75]. © 2003 National Academy of Sciences, USA.)

transistor features (i.e. an increase in drain-source current) with increasing gate bias, without any detailed detection limit analysis (Fig. 10b), they offer a general self-assembly strategy which can scale up one-dimensional nanomaterials into conventional sensor devices.

As well as their electronic properties, the superior optical properties of semiconductor NWs and CNTs can be exploited for biosensors. Single semiconducting CNTs can emit strong luminescence in the NIR region[77], where human tissue and biological fluids are particularly transparent. Very recently, Barone and coworkers[78] have made optical biosensors based on SWNTs that were first noncovalently functionalized with GOD enzyme. Electroactive mediators, such as potassium ferricyanide, $K_3Fe(CN)_6$, irreversibly adsorb on the CNT surface and shift the Fermi levels into the valence bands, then quench the CNT emission after photoexcitation. Such absorbed electroactive species could react selectively with a target analyte to modulate the fluorescence of CNTs. For example, $Fe(CN)_6^{3-}$ mediators are partially reduced by H_2O_2, creating a useful sensing application (Fig. 11a). Based on this

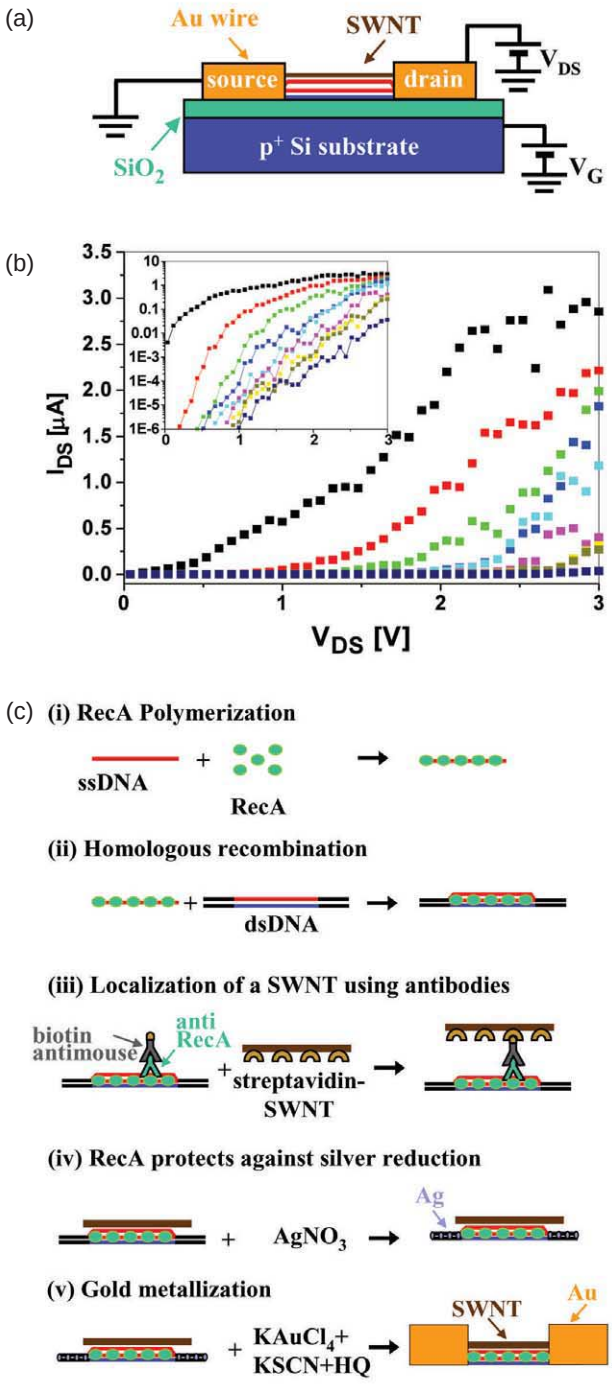

Fig. 10 (a) Schematic representation of the electrical measurement circuit. (b) Drain-source current (I_{DS}) versus drain-source bias (V_{DS}) for different values of gate bias (V_G). The inset depicts the same data on a logarithmic scale. (c) Assembly procedure of a DNA-templated FET and wires contacting it. (Reprinted with permission from[76]. © 2003 AAAS.)

idea, the assembled system was tested for the reaction of β-D-glucose to D-glucono-1,5-lactone with a H_2O_2 coproduct catalyzed by GOD. The fluorescence emission of the CNTs (λ_{max} = 994 nm) responds to the local glucose concentration

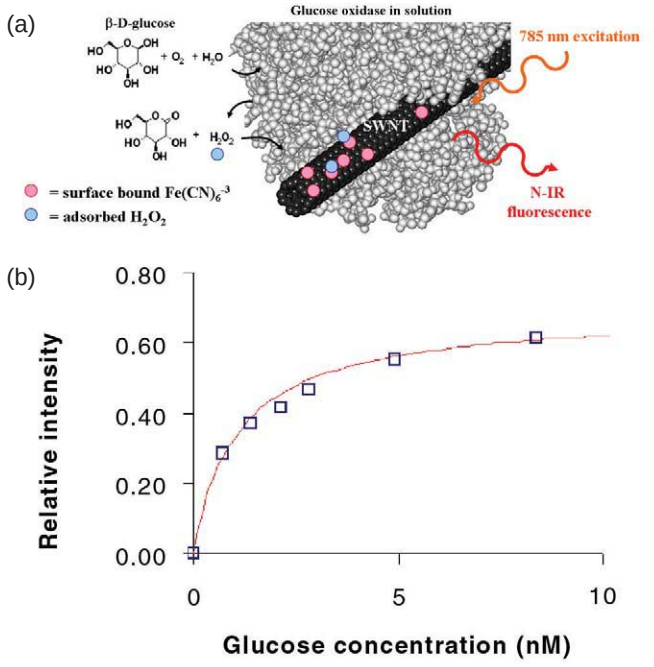

Fig. 11 Glucose detection using a CNT optical sensor. (a) Reaction at the enzyme converts glucose to gluconolactone, with the H_2O_2 coproduct detected by interaction with $Fe(CN)_6^{3-}$ functional groups on the exposed nanotube surface between enzyme monomers. (b) The response function relates the normalized intensity to the local glucose concentration in the range of blood glucose detection with a type I absorption isotherm. (Reprinted with permission from[78].)

and has a detection limit of 34.7 μM (Fig. 11b). One obvious advantage of the NIR signaling from this device is its potential for implantation into thick tissue or whole-blood media, where the signal may penetrate up to several centimeters.

Fluorescent semiconductor QDs can be used for optical nanosensing with the advantages of easy preparation, high brightness and purity of luminescence, and a broad and easily adjustable scale of luminescence. Compared with QDs, however, one-dimensional semiconductor NWs with large surface area offer a unique opportunity to improve the sensitivity of biosensors.

An example of the assembly of CdTe NWs building blocks through bioconjugation has been demonstrated by Wang *et al.*[79], in which CdTe NWs in aqueous solution are assembled with complementary connectors (either antigen-antibody and biotin-streptavidin). Cross-bar and end-to-side connections are the dominant assembly methods (Fig. 12). The formation of conjugate complexes is confirmed by FRET between NWs with different emission wavelengths, also demonstrating the potential for biosensing.

So far, most studies have focused on functionalization and immobilization of biomolecules on CNTs for characterization,

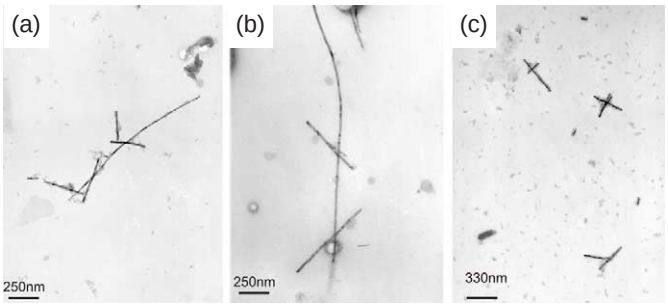

Fig. 12 Transmission electron microscopy images of assembled building blocks of (a, b) NW-biotin + NW-streptavidin, and (c) NW-biotin + streptavidin. (Reprinted with permission from[79]. © 2005 American Chemical Society.)

manipulation, separation, and device applications such as biosensors. Recent research also shows that semiconductor CNTs can be applied in bioimaging and even drug delivery[80-82]. Interesting work reported recently demonstrates that CNTs can be used as transporters for delivering small molecules or proteins into cells[83]. CNTs modified with fluorescein (Fig. 13(top), **2**) successfully enter cells through endocytosis, after which the interior of the cells exhibits green emission from the dye (Fig. 13(left)). Fluoresceinated proteins as big as streptavidin (MW ≈ 60 kD), after coupling to CNTs through conventional 1-ethyl-3-(3-dimethylaminopropyl)-carbodiimide (EDC) and biotin-streptavidin reactions (Fig. 13(top), **4**), can be transported into human promyelocytic leukemia (HL60) cells via the endocytosis pathway. Hence, the green luminescence emitted by fluorescein can be seen inside the cell (Fig. 13(right)). This work offers a new generation of biocompatible materials for drug, protein, and gene delivery applications. With the same goal of promoting information delivery into cells, CNTs have been utilized as 'electric needles' for localized perforation of cell membranes. Microwave-assisted enhancement of the electric field at the tip of CNTs has been shown to be an ideal method for perforation, and much higher inflow of Au NPs through the newly opened pores is observed, while still maintaining the viability of the cells[82].

Conclusion and future perspectives

This article has summarized the latest advances in the rapidly developing area of biomolecule-nanostructure hybrid systems, particularly for applications of semiconductor nanomaterials in bioimaging and sensing. The enthusiasm for applying QDs and one-dimensional nanostructures in biological systems is justified by their unique optical and electrical properties.

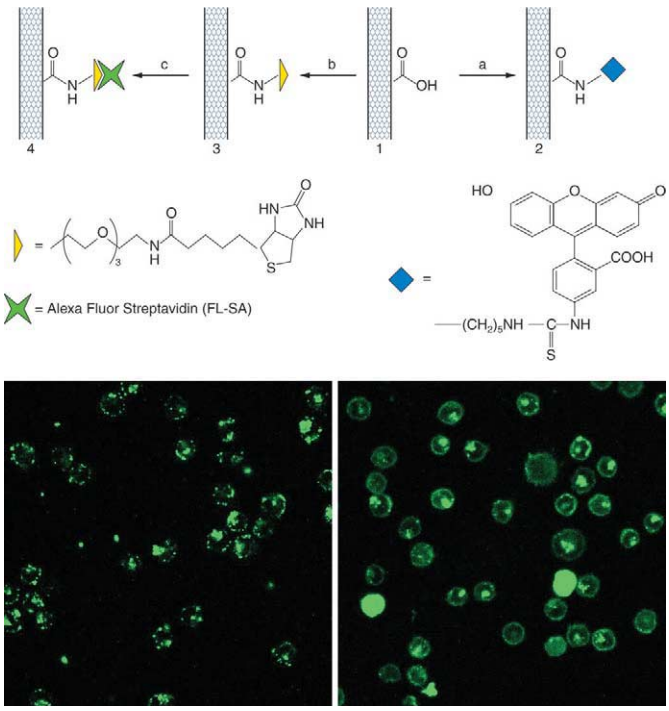

*Fig. 13 (top) Schematic of various SWNT conjugates: (a) EDC, 5-(5-aminopentyl)thioureidyl fluorescein, phosphate buffer; (b) EDC, biotin-LC-PEO-amine, phosphate buffer; and (c) fluoresceinated streptavidin. Confocal images of cells after incubation in solutions of SWNT conjugates: (left) after incubation in **2**, (right) after incubation in a mixture of **4** (green due to streptavidin) and the red endocytosis marker FM 4-64 at 37°C (image shows fluorescence in the green region only). (Reprinted with permission from[83]. © 2004 American Chemical Society.)*

Despite the popularity of QDs as luminescent labels for multimodal imaging and contrast agents, most of the colloids currently used are synthesized in the organic phase and are only soluble in nonaqueous solutions, let alone any considerations of biocompatibility. Surface modification with species such as mercaptoacetic acid, growth of a thin silica layer on the NPs, or wrapping with macromolecules facilitates aqueous solubility[58,84]. Water-soluble nanocrystals with good size distribution, high quantum yield, and defined chemical moieties are highly desirable, as are those that also meet requirements for 'green' preparation and application to deal with increasing environmental concerns. In general, QDs prepared in the aqueous phase show lower luminescence efficiency because of the low reaction temperature, and various strategies have attempted to enhance photoemission[85-90]. Recently, Wang *et al.*[91] reported that aqueous citrate-stabilized CdSe/CdS core/shell NPs can achieve a quantum yield of 60% through photoactivation – the highest reported quantum efficiency for aqueous nanocrystals. Simplicity in synthesis of photoactivable CdSe/CdS NPs, as well as the tunability and high intensity of their emission, provide important advantages over recombinant fluorescent proteins that are often used for *in vivo* studies of intracellular protein dynamics[90].

Although the application of QDs in biotechnology is compelling, they are unlikely to totally replace traditional organic dyes as biological labels, because of their much higher cost and an order of magnitude larger size. However, their capability for single-molecule and multiplexed detection, as well as real-time imaging, has secured their position as a viable technology in biological science. Other research directions using QDs together with some metal nanomaterials include the combination of nanocrystal imaging agents with therapeutic agents. Not only would this allow tracking of pharmacokinetics, but also diseased tissue could be treated and monitored simultaneously and in real time. The potential activity of nanomaterials as therapeutic agents has been demonstrated by several research groups[92-94]. This pioneering work is bridging the gap between nanotechnology and biomedicine and we anticipate the thrilling impact of nanosized colloids on medical science in the near future.

The use of one-dimensional nanostructures, like NWs and CNTs, as nanocircuitry elements is another popular research direction. Biomaterials linked to NWs and CNTs may be used as detecting probes as well as binding elements for specific linkage of these one-dimensional nanomaterials into addressable structures[76,95-97]. In addition, the use of biomolecules as templates for constructing metal contacts may be another major advance. The concept of using NW or CNT FETs modified with receptors or ligands for specific detection can be extended in many directions, such as sensing Ca ions, a key activating component for muscle contraction[28]. Distinct from Si NWs and CNTs, water-soluble fluorescent semiconducting CdTe NWs have recently been prepared via self-organization of NPs[39]. This is not only a breakthrough in synthesis of one-dimensional nanostructures, but also brings brand-new elements into bionanotechnology. These CdTe NWs, with high quantum yield and desired surface functional ligands, have been shown to exhibit sensing capability[66,79]. From the above discussion, we can see that the combination of the electrical and optical properties of one-dimensional nanostructures with the recognition features of biomolecules will provide a bright opportunity for scientists and engineers to create a new area of nanobiotechnology. NT

REFERENCES

1. Mulvaney, P., *Langmuir* (1996) **12** (3), 788
2. Bruchez, M., *et al., Science* (1998) **281**, 2013
3. Brus, L., *Appl. Phys. A* (1991) **53** (6), 465
4. Shipway, A. N., *et al., Chem. Phys. Chem.* (2000) **1** (1), 18
5. Daniel, M. C., and Astruc, D., *Chem. Rev.* (2004) **104** (1), 293
6. Alvarez, M. M., *et al., J. Phys. Chem. B* (1997) **101** (19), 3706
7. Hicks, J. F., *et al., J. Am. Chem. Soc.* (2001) **123** (29), 7048
8. Khairutdinov, R. F., *Colloid J.* (1997) **59** (5), 535
9. Hicks, J. F., *et al., J. Am. Chem. Soc.* (2002) **124** (44), 13322
10. Chen, S., and Murray, R. W., *J. Phys. Chem. B* (1999) **103** (45), 9996
11. Hicks, J. F., *et al., J. Phys. Chem. B* (2002) **106** (32), 7751
12. Trindade, T. *et al., Chem. Mater.* (2001) **13** (11), 3843
13. Schwerdtfeger, P., *et al., Angew. Chem. Int. Ed.* (2003) **42** (17), 1892
14. Gangopadhyay, R., and De, A., *Chem. Mater.* (2000) **12** (3), 608
15. Clapp, A. R., *et al., J. Am. Chem. Soc.* (2004) **126** (1), 301
16. Wang, S., *et al., Nano Lett.* (2002) **2** (8), 817
17. Willner, I., *et al., Angew. Chem. Int. Ed.* (2001) **40** (10), 1861
18. Patolsky, F., *et al., J. Am. Chem. Soc.* (2003) **125** (46), 13918
19. Xiao, Y., *et al., Science* (2003) **299**, 1877
20. Elghanian, R., *et al., Science* (1997) **277**, 1078
21. Averitt, R. D., *et al., Phys. Rev. Lett.* (1997) **78** (22), 4217
22. Xia, Y., *et al., Adv. Mater.* (2003) **15** (5), 353
23. Strong, K. L., *et al., Carbon* (2003) **41** (8), 1477
24. Seo, J. W., *et al., New J. Phys.* (2003) **5**, 1
25. Kong, J., *et al., Science* (2000) **287**, 622
26. Besteman, K., *et al., Nano Lett.* (2003) **3** (6), 727
27. Li, J., *et al., Nano Lett.* (2003) **3** (7), 929
28. Cui, Y., *et al., Science* (2001) **293**, 1289
29. Law, M., *et al., Angew. Chem. Int. Ed.* (2002) **41** (13), 2405
30. Li, C., *et al., Appl. Phys. Lett.* (2003) **82** (10), 1613
31. Xu C., *et al., J. Am. Chem. Soc.* (2004) **126** (11), 3392
32. He, X. X., *et al., Rev. Adv. Mater. Sci.* (2003) **5** (4), 375
33. West, J. L., and Halas, N. J., *Ann. Rev. Biomed. Eng.* (2003) **5**, 285
34. Gu, H., *et al., J. Am. Chem. Soc.* (2003) **125** (51), 15702
35. Thaxton, C. S., and Mirkin, C. A., *DNA-Gold-Nanoparticle Conjugates*, John Wiley & Sons, Chichester (2004)
36. Nam, J. M., *et al., Science* (2003) **301**, 1884
37. Katz, E., and Willner, I., *Angew. Chem. Int. Ed.* (2004) **43**, 6042
38. Rosenthal, S. J., *et al., Nat. Biotechnol.* (2001) **19** (7), 621
39. Tang, Z., *et al., Science* (2002) **297**, 237
40. Wu, X., *et al., Nat. Biotechnol.* (2003) **21** (1), 41
41. Chan, W. C., and Nie, S., *Science* (1998) **281**, 2016
42. Dahan, M., *et al., Science* (2003) **302**, 442
43. Lidke, D. S., *et al., Nat. Biotechnol.* (2004) **22** (2), 198
44. Hoshino, A., *et al., Biochem. Biophys. Res. Commun.* (2004) **314** (1), 46
45. Ballou, B., *et al., Bioconjugate Chem.* (2004) **15** (1), 86
46. Gao, X., *et al., Nat. Biotechnol.* (2004) **22** (8), 969
47. Parak, W. J., *et al., Adv. Mater.* (2002) **14** (12), 882
48. Pellegrino, T., *et al., Differentiation* (2003) **71** (9-10), 542
49. Voura, E. B., *et al., Nat. Medicine* (2004) **10** (9), 993-998
50. Dubertret, B., *et al., Science* (2002) **298**, 1759
51. Lim, Y. T., *et al., Mol. Imaging* (2003) **2** (1), 50
52. Rogach, A. L., *et al., Chem. Mater.* (2000) **12** (6), 1526
53. Du, H., *et al., Nano Lett.* (2002) **2** (11), 1321
54. Kan, S., *et al., Nat Mater.* (2003) **2** (3), 155
55. Kim, S., *et al., Nat. Biotechnol.* (2004) **22** (1), 93
56. Oldenburg, S. J., *et al., Chem. Phys. Lett.* (1998) **288** (2-4), 243
57. Copland, J. A., *et al., Mol. Imaging Biol.* (2001) **6** (5), 341
58. Willard, D. M., *et al., Nano Lett.* (2001) **1** (9), 469
59. Goldman, E. R., *et al., Anal. Chem.* (2002) **74** (4), 841
60. Medintz, I. L., *et al., Nat. Mater.* (2003) **2** (9), 630
61. Medintz, I. L., *et al., Bioconjugate Chem.* (2003) **14** (5), 909
62. Goldman, E. R., *et al., Anal. Chem.* (2004) **76** (3), 684
63. Medintz, I. L., *et al., J. Am. Chem. Soc.* (2004) **126** (1), 30
64. Bart, J. C., *et al., Sens. Actuators B* (1997) **39** (1-3), 411
66. Wargnier, R., *et al., Nano Lett.* (2004) **4** (3), 451
66. Lee, J., *et al., Nano Lett.* (2004) **4** (12), 2323
67. Pardo-Yissar, V., *et al., J. Am. Chem. Soc.* (2003) **125** (3), 622
68. Joseph, Y., *et al., Sens. Actuators B* (2004) **98** (1-3), 188
69. Joseph, Y., *et al., J. Phys. Chem. B* (2003) **107** (30), 7406
70. Pinna, N., *Angew. Chem. Int. Ed.* (2004) **43** (33), 4345
71. Hahm, J. I., and Lieber, C. M., *Nano Lett.* (2004) **4** (1), 51
72. Li, Z., *et al., Nano Lett.* (2004) **4** (2), 245
73. Patolsky, F., *et al., Proc. Natl. Acad. Sci. USA* (2004) **101** (39), 14017
74. Collins, G., *et al., Science* (2000) **287**, 1801
75. Chen, R. J., *et al., Proc. Natl. Acad. Sci. USA* (2003) **100** (9), 4984
76. Keren, K., *et al., Science* (2003) **302**, 1380
77. O'Connell, M. J., *et al., Science* (2002) **297**, 593
78. Barone, W., *et al., Nat. Mater.* (2005) **4** (1), 86
79. Wang, Y., *et al., Nano Lett.* (2005) **5** (2), 243
80. Cherukuri, P., *J. Am. Chem. Soc.* (2004) **126** (48), 15638
81. Pantarotto, D., *et al., Chem. Commun.* (2004) **1,** 16
82. Rojas-Chapana, J. A., *et al., Nano Lett.* (2004) **4** (5), 985
83. Kam, N. W., *et al., J. Am. Chem. Soc.* (2004) **126** (22), 6850
84. Aldana, J., *et al., J. Am. Chem. Soc.* (2001) **123** (38), 8844
85. Bol, A. A., *et al., J. Phys. Chem. B* (2001) **105** (42), 10197
86. Danek, M., *et al., Chem. Mater.* (1996) **8** (1), 173
87. Mews, A., *et al., J. Phys. Chem. B* (1994) **98** (3), 934
88. Rogach, A. L., *et al., Chem. Mater.* (2000) **12** (9), 2676
89. Wang, Y., *et al., J. Am. Chem. Soc.* (2003) **125** (10), 2830
90. Patterson, G. H., *et al., Science* (2002) **297**, 1873
91. Wang, Y., *et al., J. Phys. Chem. B* (2004) **108** (40), 15461
92. Bakalova, R., *et al., Nano Lett.* (2004) **4** (9), 1567
93. Samia, A. C. S., *et al., J. Am. Chem. Soc.* (2003) **125** (51), 15736
94. Hirsch, L. R., *et al., Proc. Natl. Acad. Sci. USA* (2003) **100** (23), 13549
95. Caswell, K. K., *et al., J. Am. Chem. Soc.* (2003) **125** (46), 13914
96. Connolly, S., and Fitzmaurice, D., *Adv. Mater.* (1999) **11** (14), 1202
97. Alivisatos, A. P., *et al., Nature* (1996) **382**, 609